Single-ion anisotropy in Mn-doped diluted magnetic semiconductors

Adrien Savoyant, A Stepanov, R Kuzian, C Deparis, C Morhain, K Grasza

Single-ion anisotropy in Mn-doped diluted magnetic semiconductors

A. Savoyant and A. Stepanov
IM2NP, CNRS UMR 6242, FST, Université Paul Cézanne, F-13397 Marseille Cedex 20, France

R. Kuzian
Institute for Materials Science, Krzhizhanovskogo 3, 03180 Kiev, Ukraine

C. Deparis and C. Morhain
Centre de Recherches sur l'Hétéroépitaxie et ses Applications, CNRS, F-06560 Valbonne, France

K. Grasza
Institute of Physics, Polish Academy of Sciences, al. Lotnikow 32/46, 02-668 Warsaw, Poland

(Received 30 June 2009; revised manuscript received 7 August 2009; published 10 September 2009; corrected 11 September 2009)

Motivated by recent developments in spintronics, we propose an explanation of the single-ion anisotropy of Mn-doped diluted magnetic semiconductors using as an example high-quality ZnO:Mn thin films for which *X*-band electron-paramagnetic-resonance studies were performed. We derive an analytic formula for the axial parameter *D* and we prove its validity by the exact diagonalization method. We demonstrate a quantitative agreement between the experimental data and our model. These results bring insights into a long-standing problem of single-ion anisotropy in magnetic solids.

DOI: 10.1103/PhysRevB.80.115203 PACS number(s): 75.50.Pp, 71.20.Nr, 75.30.Gw, 76.30.Fc

I. INTRODUCTION

The efficiency of conventional microelectronics is quantum mechanically limited due to the continual reduction in the size of its components rapidly approaching nanoscale dimensions. Spin electronics or spintronics, which has emerged as a alternative technology that manipulates the electron spin rather than its charge, opens fascinating routes for information processing and storage.[1] Currently, *metallic* ferromagnetic (FM) materials are used as spin-polarization components in most spintronic devices such as a reading head for hard disk drives, MRAM, etc. This hinders their compatibility with existing semiconductors technology. An appropriate solution would be a FM semiconductor.

Diluted magnetic semiconductors (DMS) and, in particular, manganese-doped DMS, which combine favorably ferromagnetic and semiconducting properties, have become recently the subject of considerable interest as promising materials for spin electronics.[2–4]

Manipulating the spin of an electron implies a proper control of its spin orientation. When magnetic field is applied to a spin system, the magnetization does not follow exactly the magnetic field direction. Instead it is aligned in a particular direction imposed by the *magnetic anisotropy*. Since the control of magnetic anisotropy is proved to be essential in fabricating of practical semiconductor spintronic devices,[4] it is of fundamental importance to improve our understanding of its microscopic mechanisms.

In the present paper we examine the nature of the single-ion anisotropy (SIA) of Mn-doped DMS illustrating our approach by *X*-band electron-paramagnetic-resonance (EPR) studies on high-quality ZnO:Mn thin films. A particular focus is placed on the axial SIA of Mn^{2+} (^6S-state ion) because at low TM concentration, characteristic for DMS, it plays an important role.[5]

The commonly accepted way of describing of SIA is the spin-Hamiltonian (SH) formalism which provides a simple phenomenological description of measured magnetic properties, EPR spectra, etc., by using of a limited number of parameters. The challenge is then to compute these parameters. Various perturbative treatments of SH parameters for *S* ions within crystal-field (CF) theory were proposed during last five decades and are summarized in Refs. 6 and 7. In particular, the SIA of *S* ions in *cubic crystals*, including tetrahedral II-VI compounds, was discussed in detail[6] and a model describing the evolution of the cubic SH parameter, *a*, in series of II-VI compounds ($ZnX, X=S, Se, Te$) was suggested.

As far as the axial parameter *D* concerns the situation is much less clear and, quite surprisingly, a reliable theory is still lacking. The expression for *D* (Ref. 6), cited in literature, suffers from ambiguous notations so that it is difficult to establish its validity (see, for example, discussion in Ref. 8). Moreover and much more importantly, the physical content of previously formulated models cannot be considered as satisfactory and for the most part this is due to a poor treatment of hybridization contribution to crystal-field parameters.

In order to remedy this situation and to gain more insight into the origin of axial SIA we develop a detailed crystal-field-like model that considers two sources of *D*: electrostatic interaction between *S* ion and surrounding ligands, and *p-d* hopping from ligands to *S* ion (hybridization). Then we treat the Hamiltonian for the $3d^5$ configuration using the exact diagonalization method and by developing a perturbative approach which enable us to obtain explicit analytic formula for *D*. Finally, we perform a quantitative comparison between the experimental data and our model and we show quite generally that the problem of axial SIA requires further development of a hybridization theory.

II. EXPERIMENTAL DETAILS

ZnO:Mn has attracted much attention as a candidate for a room-temperature FM semiconductor, nevertheless its magnetic properties still remain highly controversial. Both FM and paramagnetic phases were detected in ZnO:Mn thin films.[9–13] Therefore, high-quality single-crystalline thin films are needed to clarify these issues.

The experiments were carried out on a set of *c*-oriented $Zn_{1-x}Mn_xO$ ($x=0.0014-0.018$) thin films grown onto *c*-sapphire substrates by plasma-assisted molecular-beam epitaxy. The film thickness was about 1.7 μm. For the growth, oxygen was activated in a RIBER rf-plasma cell equipped with a high-purity quartz cavity, while elemental, 6N purity grade Zn and Mn were evaporated using RIBER Knudsen cell designed for the growth of oxides. The conductivity of the films was *n* type, with a residual carrier concentration $n_e < 10^{16}$ cm^{-3}. The growth temperature was regulated at 570 °C (i.e., 60 °C higher than the optimal growth temperature for ZnO) as higher temperatures were found to result in an improved crystalline quality of the epilayers and minimized twist. Such improvement is attested by lower full widths at half maximum on the high-resolution x-ray diffraction scans for symmetric, asymmetric as well as oblique directions. Two-dimensional (2D) growth was obtained from the very beginning of the growth as attested by the streaky reflection high-energy electron-diffraction patterns, which often displayed a marked 3×3 reconstructed surface. While the surface of the samples roughens with time, it was however possible to maintain a 2D growth for the whole duration of the growth for the two samples having the lowest Mn content. The Mn composition *x* of the studied samples was estimated by energy-dispersive x-ray microanalysis and by secondary-ion mass spectrometry and was found to be uniform. In addition to thin-film samples a single crystal of ZnO very lightly doped by Mn with $x \simeq 10^{-6}$ was also used in experiments as a reference sample.

The ^6S ground state of Mn^{2+} at a trigonally distorted tetrahedral site of the ZnO lattice is described by the following $S=5/2$ spin Hamiltonian[14]

$$\hat{H}_{\text{spin}} = \frac{D}{3}O_2^0(S) + \frac{F-a}{180}O_4^0(S) - \frac{a\sqrt{2}}{9}O_4^3(S) + A\mathbf{S}\cdot\mathbf{I} + g\beta\mathbf{H}\cdot\mathbf{S}, \quad (1)$$

where O_k^q are Steven's operators, *D* and *F* are the second- and fourth-order axial parameters, respectively, *a* is the cubic parameter, *g* is the isotropic *g* factor, and *A* is the hyperfine constant.

The *X*-band EPR spectra were recorded using a Bruker EMX spectrometer equipped with a standard TE_{102} cavity and a continuous helium-flow cryostat that allows temperature scans between 4 and 300 K. The films with an area of 3×3 mm^2 were mounted on a quartz-rod sample holder. The angle between the *c* axis of the films and the direction of the static magnetic field *H* was controlled by a goniometer with a precision better than $\pm0.25°$.

In Fig. 1 representative EPR spectra collected on $Zn_{1-x}Mn_xO$ films with different Mn content are shown. It is important to note that the high quality of our films allows us

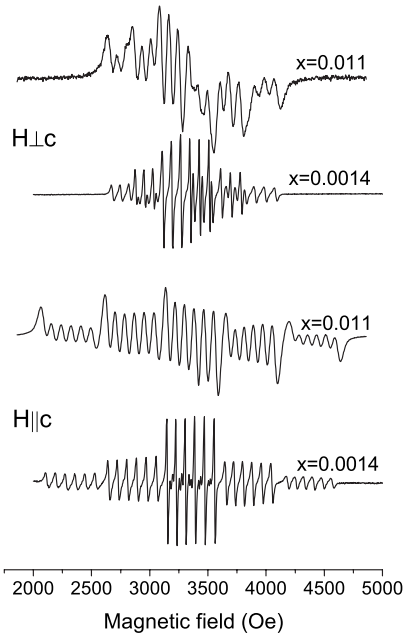

FIG. 1. *X*-band EPR spectra taken on $Zn_{1-x}Mn_xO$ films with different Mn content at 6 K for $H \| c$ and $H \perp c$.

to follow all 30 components of Mn^{2+} spectrum for all studied Mn concentrations and, therefore, to ensure the absence of any secondary impurity phases. For each particular value of *x* the EPR spectrum was fitted using *easyspin* toolbox[15] in order to obtain the above-defined parameters of the spin Hamiltonian. We found that in our samples $D=-710\pm5$ MHz for $x=0.0014$ (Ref. 16) and that *D* shows up a weak increase of about 5% going from $x=0.0014$ to $x=0.018$. One can compare these results with recently reported EPR data on ZnO:Mn films[17] where an opposite trend was observed, i.e., a decrease in *D* with increasing of *x*. Two other parameters $a-F=18\pm3$ MHz and $A=225\pm5$ MHz (Ref. 16) exhibit only a small variation, within an experimental error, in the whole range of *x*. The measured effective *g* factor is found to be *x* dependent and ranging from 2.0016 at $x=0.0014$ to 1.994 at $x=0.018$. Simple estimates show that this *g*-factor shift can be explained by the growing role of the sample demagnetization field at low temperature. Hereafter, for the sake of concreteness, we discuss the SH parameters of the sample with $x=0.0014$.

III. MODEL

In order to calculate parameters of the spin Hamiltonian (1) we use the model which includes the Hamiltonian of isolated Mn^{2+} ion (the Coulomb repulsion between *d* electrons $\hat{H}_C^0$ and the spin-orbit (SO) coupling $\hat{H}_{\text{SO}}^0$), electrostatic interaction between *d* electrons and ligands and *p*-*d* hopping between ligand *p* and Mn *d* states. A canonical Schrieffer-Wolff-type transform[18] reduce this model to an effective single-ion CF Hamiltonian[19]

$$\hat{H} = \hat{H}_C + \hat{H}_{\text{SO}} + \hat{H}_{\text{CF}}, \quad (2)$$

$$\hat{H}_{\mathrm{CF}} = -\frac{2}{3}B_4^0(\hat{O}_4^0 - 20\sqrt{2}\hat{O}_4^3) + B_2'\hat{O}_2^0 + B_4'\hat{O}_4^0, \qquad (3)$$

here the Steven's operators $\hat{O}_k^q$ are the polynomials of the one-electron orbital angular moment $\hat{l}$. The expressions for the CF parameters B_k^q can be written as a sum of two terms: $B_k^q = B_{k,e}^q + B_{k,h}^q$, where $B_{k,e}^q$ is an electrostatic contribution and $B_{k,h}^q$ is a hybridization one (see for details Refs. 19 and 20). The latter represents the influence of *p-d* hybridization on the CF parameters in the perturbation theory with respect to t_{pdm}/Δ_{pd} $(m=\sigma,\pi)$, where t_{pdm} are the *p-d* hoppings and Δ_{pd} is the charge-transfer energy. The hoppings are expressed by Harrison parametrization.[21] Note that the canonical transformation leads also to the reduction in Coulomb and spin-orbit interaction parameters $\xi \approx k\xi_0$, $B \approx k^2 B_0$, and $C \approx k^2 C_0$, where ξ_0, B_0, and C_0 are free-ion SO coupling and Racah parameters,[22] respectively. The reduction factor was given in Ref. 19 [Eq. (26)], where our approach was applied to the SIA calculation of Co^{2+} impurity ($3d^7$ configuration) in ZnO.

We diagonalize the matrix of the Hamiltonian $\hat{H}$ within the basis set of Mn^{2+}-ion $3d^5$ configuration. The matrix dimensions are 252×252. Numerical diagonalization was done by a FORTRAN program. Program's entries are: the crystallographic data (we use $a=3.252$ Å, $c=5.203$ Å, and $u=0.383$, which correspond to the sample with $x=0.0014$), the free-ion parameters $B_0=900$ cm^{-1}, $C_0=3300$ cm^{-1}, and $\xi_0=400$ cm^{-1}, the photoemission data on ZnO:Mn, $\Delta_{pd}=6.5$ eV (Ref. 23) and $t_{pd\sigma}=-1.62$ eV.

In the absence of a magnetic field, the ground-state ^6S splits into the three twofold-degenerate levels. The energy differences between successive levels, ΔE_1, ΔE_2 extracted from the numerical calculations were used to estimate D using the well-known formulas.[14]

The ground state ^6S has zero matrix elements of the CF with any other d^5 multiplet. The energy that separates the ground state and the first excited state is much larger then the parameters of the SO and CF interactions. So, very small admixture of the excited states by SO interaction determines the spin-Hamiltonian (1) parameters. By treating $\hat{H}_{\mathrm{SO}}$ and $\hat{H}_{\mathrm{CF}}$ as perturbations of $\hat{H}_C$ (H. Watanabe's approach[6,24]) we have rederived the fourth-order expression for D,

$$D^{(4)} = \frac{189B_2'\xi^2}{10\mathcal{P}^2\mathcal{D}}(\xi - B_2') + \frac{1680B_4'\xi^2}{\mathcal{P}^2\mathcal{G}}(4B_4^0 - 3B_4'), \qquad (4)$$

where $\mathcal{P}=7(B+C)$, $\mathcal{D}=17B+5C$, and $\mathcal{G}=10B+5C$ are the energy differences between the ground state ^6S and, ^4P, ^4D, and ^4G excited levels, respectively. We have checked that D of Eq. (4), within a few percent, agrees with the exact diagonalization results, in the range of used CF parameters.

IV. RESULTS AND DISCUSSION

We are now at a point to make a quantitative comparison between our theoretical model and the obtained data. One can do this in two steps. First, we will fix the single-ion parameters, B, C, and ξ and the cubic CF parameter B_4^0. The latter is estimated in the simplest CF model which includes four nearest-neighbors oxygens. Since these parameters are relevant for optical properties, their choice is often dictated by an analysis of optical spectra of a particular $3d$ ion being studied. However, in the case on ZnO, not much data is available in literature regarding the excited-level energies of Mn^{2+}. One of the reasons is that Mn^{2+} in ZnO exhibits a broad intraionic absorption band above 2.2 eV *without a fine structure*, which is characterized by a surprisingly large absorption coefficient for a spin-forbidden transition.[25] While there are still doubts as to the origin of this absorption band, its observation is compatible with the results of calculations made within a configuration-interaction (CI) model[23] which gives the energies of $^4T_1$, $^4T_2$, ^4E, and $^4A_1$ states, between 2.55 and 2.99 eV (see Table I). Another source of information is optical spectra of Mn^{2+} in ZnS which were studied in great details (see, for example, Ref. 26) and which, given the proximity of these two materials, ZnO and ZnS, can help to fix the CF parameters of ZnO. According to Richardson and Janssen[26] the energies of above cited four levels in ZnS lie between 2.34 and 2.67 eV, i.e., lower than the energies obtained in CI calculations. Our model predicts the excited-level energies shown in the second column of Table I which are closer to the beginning of the observed absorption band 2.2 eV than CI calculations. Note also that we do not use any adjustable parameter and that presented data are not sensitive to the choice of anisotropy constants B_2' and B_4'.

TABLE I. Energies of Mn^{2+} excited states in ZnO in eV obtained by the exact diagonalization for $Dq(12B_4^0)=-562$ cm^{-1}, other parameters are defined in the text, as compared to the calculations within CI model (Ref. 23) and optical data on ZnS:Mn (Ref. 26).

Excited states	This work	CI calc.	ZnS optics
$^4T_1$	2.21	2.55	2.34
$^4T_2$	2.59	2.85	2.49
^4E	2.73	2.97	2.67
$^4A_1$	2.73	2.99	2.67

Now, in order to estimate D according to formula (4) we need to compute B_2' and B_4'. This is a difficult task which, contrary to B_4^0 computation, involve a summation of various ligand contributions, i.e., one has to know the crystal field created by first, second, third, etc., successive neighbors of Mn^{2+}. While special attention should be paid to the convergence of contributions to B_2' because it is a conditional one, the necessary summation can be performed for the electrostatic part of B_n', by choosing an appropriate neutral group of ions in successive spherical shells.

The difficulties emerge when one attempts to include the hybridization contribution from the whole crystal. For this purpose we need, in fact, the solution of realistic full many-body impurity problem in a crystal. It demands the summation of higher orders of perturbation-theory expansion which accounts for multiple hoppings in real space or multiple integrations over Brillouin zone in **k** space. In any case, the simplicity of analytic form of the second order of perturbation theory will be lost. Such investigation, which requires also a precise knowledge of the electronic structure of host

TABLE II. CF parameters computed in different models and D obtained according to perturbative formula (4).

Parameter	4 ligands	5 ligands	Summation
B_2'	82.6 cm^{-1}	−65.7 cm^{-1}	60.5 cm^{-1}
B_4'	4.1 cm^{-1}	5.9 cm^{-1}	8.1 cm^{-1}
D	−283 MHz	−698 MHz	−712 MHz
κ	1	1	2.8

crystal as well as parameters of impurity-host interactions, we leave for future work.

In order to proceed with an estimation of D we have considered three CF models. The first model, which is the simplest one, deals with a CF made by only four nearest oxygens. A main weakness of this model is that an important contribution of a hexagonal wurtzite lattice originated from distant oxygens and zincs is neglected. This means, for example, that in the case of compounds with an ideal wurtzite structure $[c/a=\sqrt{(8/3)}]$ axial SIA is zero, which is certainly not correct. In the second model we remedy this shortcoming by adding a fifth oxygen which is placed in wurtzite structure on z axis and whose z coordinate is $z=-(5/8)c$. In the third model, the electrostatic contribution to B_n' is computed by the direct lattice summation and hybridization contribution is added, multiplied by an adjustable parameter. Since, according to Eq. (4), the main contribution to D comes from B_4' we assume that $B_4'=B_{4,e}'+\kappa B_{4,h}'$, using $B_{4,h}'$ value from the first model. Therefore, κ somehow accounts for an unknown contribution coming from distant ligands. The results of calculations made according to these models are presented in Table II. As expected the first model strongly underestimates D, the second one gives D close to experimentally observed value but this coincidence is most probably fortuitous and the third one points clearly to the problem of summation of hybridization contributions. To make our conclusions more convincing we performed rough estimates of D in other two wurtzite compounds doped by Mn^{2+}, GaN, and AlN. Using the following parameters $a=3.188$ Å, $c=5.185$ Å, $u=0.377$, and $\kappa=2.8$ for GaN and $a=3.11$ Å, $c=4.98$ Å, $u=0.383$, and $\kappa=2.2$ for AlN and the photoemission data from Ref. 27 we obtain $D_{GaN}\simeq-660$ MHz and $D_{AlN}\simeq-1850$ MHz, in excellent agreement with experimental data,[8] $D_{GaN}\simeq-218-236$ G (−610−660 MHz) and $D_{AlN}\simeq-648$ G (−1814 MHz).

It is interesting to consider how D affects the magnetic properties. In all three compounds D is found to be negative which means that the magnetic "easy axis," resulting from the SIA mechanism, coincides with the c axis of wurtzite structure. If a magnetic field H applied perpendicular to this axis its strength should at least exceed the anisotropy field $H_a\simeq 2DS/g\mu_B$ in order to observe the magnetization saturation. In the case of ZnO:Mn, for example, H_a is of about 1.3 kOe. Note that this anisotropy field does not depend on Mn concentration since it has a single-ion origin. There exist other sources of magnetic anisotropy which take their origin from Mn-Mn interaction. Under p doping the ferromagnetism is observed in some Mn-doped II-VI and III-V DMS and attributed to the hole-mediated exchange interaction between Mn ions. This ferromagnetic state, in strained samples, often exhibits the magnetic anisotropy with H_a of several kOe. The mechanism of this pair anisotropy (PA), however, is fundamentally different from SIA at least in two points. First, while both mechanisms are based on p-d hybridization, in SIA the hybridization takes place between $3d$ ions and *occupied electron* bands in contrast with PA where $3d$ ions hybridized with almost *free carriers* (Zener model). Second, PA in DMS results from the p electron spin-orbit coupling whereas SIA originates from the spin-orbit coupling of $3d$ electrons. As a consequence, there exits a range of parameters such as hole concentration p, magnetization M, etc., where both of considered anisotropy mechanisms play equally important role, $H_a^{PA}\simeq H_a^{SIA}$. To see this more clearly let us assume that, H_a^{PA} scales linearly with hole concentration, $H_a^{PA}\sim p$ (Ref. 28) and with magnetization $H_a^{PA}\sim M$ whereas H_a^{SIA}, according to our model, does not depend neither on p nor on M. It is therefore evident that for some p^* or M^* SIA and PA contributions become comparable. We return now to ZnO:Mn in an attempt to get an order-of-magnitude estimate for p^* in this system. Taking typical parameters of GaAs:Mn,[29] as a starting point, and considering that in ZnO:Mn, according to magnetoptical measurements, $N_0|\alpha-\beta|\simeq 0.15$ eV,[25] i.e., an order-of-magnitude less than in GaAs:Mn, we obtain that for a ZnO:Mn sample with 3% of Mn, p^* is about of 10^{20} cm^{-3}, i.e., in the range of typical concentrations required for the ferromagnetism. Note in passing that in a commonly accepted model of DMS magnetic anisotropy[30] a SIA contribution is completely neglected. As the above analysis shows this approximation does not hold for all Mn-doped DMS.

V. CONCLUSIONS

In conclusion, we propose a model of the effective crystal field and the single-ion anisotropy which readily accounts for electrostatic and hybridization contributions and which provides a reasonable interpretation of the EPR data obtained on ZnO:Mn films and other Mn-doped DMS. We argue that a comprehensive understanding of single-ion anisotropy mechanisms requires further development of p-d hybridization theory in magnetic materials. Clearly, this last problem goes far beyond the context of DMS physics.

ACKNOWLEDGMENTS

This work was partly supported by the CNRS-NASU program PICS (Contract No. 4767). Discussions with S. M. Ryabchenko, A. M. Daré, and R. Hayn are gratefully acknowledged.

[1] M. A. Nielsen, M. R. Dowling, M. Gu, and A. C. Doherty, Science **311**, 1133 (2006).
[2] H. Ohno, Science **281**, 951 (1998).
[3] I. Žutić, J. Fabian, and S. Das Sarma, Rev. Mod. Phys. **76**, 323 (2004).
[4] Y. Ohno, D. K. Young, B. Beschoten, F. Matsukura, H. Ohno, and D. D. Awschalom, Nature (London) **402**, 790 (1999); T. Dietl, H. Ohno, F. Matsukura, J. Cibert, and D. Ferrand, Science **287**, 1019 (2000).
[5] O. M. Fedorych, E. M. Hankiewicz, Z. Wilamowski, and J. Sadowski, Phys. Rev. B **66**, 045201 (2002).
[6] Yu Wan-Lun and Zhao Min-Guang, Phys. Rev. B **37**, 9254 (1988).
[7] Yu Wan-Lun and C. Rudowicz, Phys. Rev. B **45**, 9736 (1992).
[8] T. Graf, M. Gjukic, M. Hermann, M. S. Brandt, M. Stutzmann, and O. Ambacher, Phys. Rev. B **67**, 165215 (2003).
[9] M. Venkatesan, C. B. Fitzgerald, J. G. Lunney, and J. M. D. Coey, Phys. Rev. Lett. **93**, 177206 (2004).
[10] K. R. Kittilstved, N. S. Norberg, and D. R. Gamelin, Phys. Rev. Lett. **94**, 147209 (2005).
[11] M. H. Kane, K. Shalini, C. J. Summers, R. Varatharajan, J. Nause, C. R. Vestal, Z. J. Zhang, and I. T. Ferguson, J. Appl. Phys. **97**, 023906 (2005).
[12] J. R. Neal, A. J. Behan, R. M. Ibrahim, H. J. Blythe, M. Ziese, A. M. Fox, and G. A. Gehring, Phys. Rev. Lett. **96**, 197208 (2006).
[13] A. J. Behan, A. Mokhtari, H. J. Blythe, D. Score, X.-H. Xu, J. R. Neal, A. M. Fox, and G. A. Gehring, Phys. Rev. Lett. **100**, 047206 (2008).
[14] A. Abragam and B. Bleaney, *Electron Paramagnetic Resonance of Transition Ions* (Clarendon, Oxford, 1970).
[15] S. Stoll and A. Schweiger, J. Magn. Reson. **178**, 42 (2006).
[16] P. R. Dorain, Phys. Rev. **112**, 1058 (1958).
[17] M. Diaconu, H. Schmidt, A. Pöppl, R. Böttcher, J. Hoentsch, A. Klunker, D. Spemann, H. Hochmuth, M. Lorenz, and M. Grundmann, Phys. Rev. B **72**, 085214 (2005).
[18] J. R. Schrieffer and P. A. Wolff, Phys. Rev. **149**, 491 (1966).
[19] R. O. Kuzian, A. M. Daré, P. Sati, and R. Hayn, Phys. Rev. B **74**, 155201 (2006).
[20] M. D. Kuz'min, A. I. Popov, and A. K. Zvezdin, Phys. Status Solidi B **168**, 201 (1991).
[21] W. A. Harrison, *Electronic Structure and the Properties of Solids* (Freeman, San Francisco, 1980).
[22] G. Racah, Phys. Rev. **62**, 438 (1942).
[23] T. Mizokawa, T. Nambu, A. Fujimori, T. Fukumura, and M. Kawasaki, Phys. Rev. B **65**, 085209 (2002).
[24] H. Watanabe, Prog. Theor. Phys. **18**, 405 (1957).
[25] W. Pacuski, Ph.D. thesis, Université Joseph Fourier, Grenoble, 2008.
[26] J. W. Richardson and G. J. M. Janssen, Phys. Rev. B **39**, 4958 (1989).
[27] J. I. Hwang, Y. Ishida, M. Kobayashi, H. Hirata, K. Takubo, T. Mizokawa, A. Fujimori, J. Okamoto, K. Mamiya, Y. Saito, Y. Muramatsu, H. Ott, A. Tanaka, T. Kondo, and H. Munekata, Phys. Rev. B **72**, 085216 (2005).
[28] M. Glunk, J. Daeubler, L. Dreher, S. Schwaiger, W. Schoch, R. Sauer, W. Limmer, A. Brandlmaier, S. T. B. Goennenwein, C. Bihler, and M. S. Brandt, Phys. Rev. B **79**, 195206 (2009).
[29] In GaAs:Mn H_a is typically of order 4–5 kOe for optimized strained films, with 5% of Mn, hole concentraion $\sim 3.5 \cdot 10^{20}$ cm^{-3} and epitaxial strain $\epsilon_{zz} \simeq 0.4\%$ (Ref. 28).
[30] T. Dietl, F. Matsukura, and H. Ohno, Phys. Rev. B **66**, 033203 (2002).